

# Design of an Electronically-Interfaced Dispatchable Power Generation Source to Facilitate Islanding and Autonomous Operation of a Distribution Network

Farid Katiraei, *Member, IEEE*, and Chad Abbey, *Student Member, IEEE*  
CANMET Energy Technology Centre - Varennes, Natural Resources Canada

**Abstract**—Planned islanding and autonomous operation of a medium voltage distribution system with high-penetration of renewable energy resources are examined in this paper. The intermittent nature and highly variable characteristics of renewable sources identify them as non-dispatchable sources that require a stiff grid and/or electric energy storages for continuous supply of electricity and reliable operation of a power distribution network. A design methodology based on characterization of the frequency-power relationship of all sources in the planned island is introduced and applied to the development of a fast-acting, dispatchable distributed energy resource (DER). The dispatchable DER is employed to quickly maintain power balance of a distribution system upon disconnection from the grid and stabilize the system operation following the islanding transients. The proposed DER is electronically-interfaced and composed of a slow-response primary source and a short-term energy storage. Design criteria aim to minimize the size of the storage while providing adequate power to compensate fluctuations of variable sources during an autonomous operation. Case studies based on the islanding of the distribution network with and without the dispatchable source are performed. The study results illustrate operating limits and power mismatch levels for which the islanded system can be sustained given specified acceptable voltage and frequency ranges.

**Index Terms**—Dispatchable source, electric energy storage, renewable energy sources, planned islanding, Microgrid.

## I. INTRODUCTION

Planned islanding and autonomous operation of part of a distribution network supplied by local distributed energy resources (DER) has recently attracted major utilities' interest worldwide, [1], [2]. The concept can potentially improve reliability and supply security of the distribution network by reducing system downtime. It also allows the utility company to perform maintenance on upstream medium/high voltage feeders without supply interruption of the low voltage customers. As the penetration depth of DERs based on alternative energy sources - particularly renewable energy technologies - increases, DER owners may demand islanding capability during the interval of a sustained grid failure and, in some cases, to enhance power quality for disturbances initiated on the main grid.

Current planned-islanding practices are based on pre-scheduling of controllable DERs to balance the power generation and consumption locally prior to disconnection from

the utility grid, [3]. This operating strategy requires close control and supervision of generation sources that limits the utility applications to specific systems with no or very low-penetration of intermittent and renewable energy sources. One solution to expand the application is to utilize electric energy storage; however, the high cost of energy storage requires optimal sizing and selection of appropriate storage technologies. Implication of advanced control strategies may also help enhance the dynamic behavior of the system, enabling the reduction of the storage size.

This paper presents the design methodologies and performance analyses of an electronically-interfaced dispatchable distributed energy resource (EID-DER) to manage the instantaneous power fluctuations and overall energy balance of a distribution network during islanding and autonomous operation. The fast-acting EID-DER is composed of a gas turbine, the primary source, and an ultracapacitor energy storage bank as the secondary source of energy generation. The ultracapacitor supplies the short-term energy requirements during start-up and/or acceleration/deceleration intervals of the comparably slow-response conventional source, i.e. gas turbine.

Ultracapacitor-based energy storage has been primarily used for hybrid electric vehicle applications, [4], to provide instantaneous energy during engine acceleration; also in dc traction systems to operate as a shock absorber to reduce voltage sags on the dc bus [5]. Recent demonstration projects, e.g. "capacitor-stabilized soft-transfer interface system" conducted by EPRI [6], and "Ultracapacitor EnergyBridge<sup>TM</sup>" technology introduced by Northern Power Systems, [7], have investigated ultracapacitor-based energy storage applications for distribution systems. However, the sizing issue and design of an efficient energy storage medium for these applications imply that in-depth analysis of the system characteristics is required.

The main contribution of this paper is the development of a design approach and an analytical method for sizing and control system design of an ultracapacitor-based dispatchable source. The proposed method is based on the investigation of the system stiffness and rate of voltage/frequency changes to determine the instantaneous real and reactive power requirements. The paper also presents dynamic performance analyses of the distribution network, during and subsequent to planned and unplanned (accidental) islanding, with and without the EID-DER.

The following topics are treated in turn. First, planned islanding control strategies based on a typical utility practice

---

Authors are with Natural Resources Canada, CANMET Energy Technology Centre-Varennes, 1615 Lionet-Boulet Blvd., Quebec, Canada, J3X 1S6, (emails: farid.katiraei@nrcan.gc.ca, chad.abbey@nrcan.gc.ca)

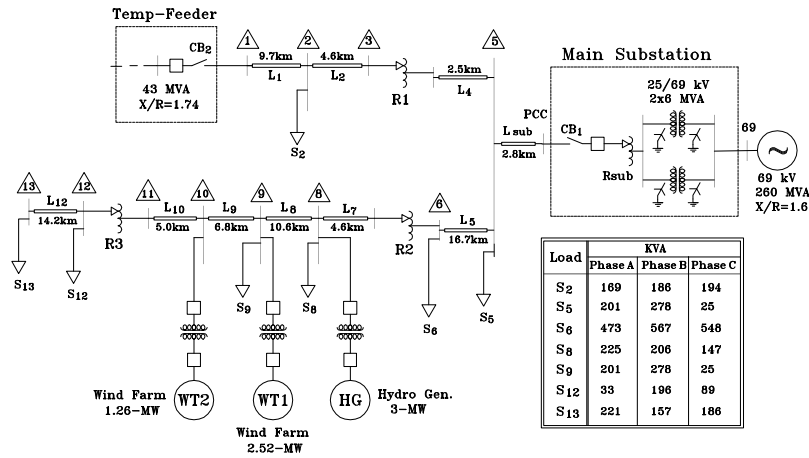


Fig. 1. One-line diagram of the 25-kV utility benchmark system of the study

using the available energy sources for a distribution network, without fast-acting DER, are described and typical ranges of voltage and frequency changes for a given disturbance are identified. Then, an analytical approach based on transfer function analysis is described and used to design the control system for the EID-DER and determine the size of the ultracapacitor storage. Transient behavior of the network and EID-DER performance for selected cases of islanding and autonomous operation at various load/generation conditions are studied and simulation results are presented to demonstrate the enhancement of the dynamic performance of the network.

## II. SYSTEM DESCRIPTION

Fig. 1 shows the one-line diagram of a 25-kV local distribution network configured downstream of a 65-kV/25-kV substation, which is denoted “main substation”. The distribution network is normally connected to the “main substation” as the point of common coupling (PCC) with the utility grid. However, in some circumstances, e.g. during maintenance periods of the “main substation” or a permanent fault on the high voltage (HV) feeder, the utility power source is temporarily switched to an adjacent 25-kV distribution feeder (temp-feeder) of a 138-kV/25-kV substation, [8]. The connection point is shown at one end of the network backbone, Node-1 in Fig. 1.

The distribution network supplies distributed load of about 4.82-MW. For simplicity, the distributed load of the network is represented by equivalent lumped values connected at seven nodes along the backbone feeder in Fig. 1. Two sets of three 660-kW and three 600-kW wind turbines with a total rated capacity of 3.78-MW, and a run-of-river hydro-power generator with peak generation of 3-MW are connected along the backbone of the distribution feeder. The wind turbines are grouped together to represent two wind farms connected at Node-9 and Node-10 in Fig. 1.

The local distributed energy resources are intermittent sources introducing daily and seasonal power fluctuations. Under strong wind conditions and high availability of water resources, there is enough power generated by the DERs to

supply the load demand of the network; in some cases excess power, reversing the power flow direction towards the grid.

## III. ISLANDING PRACTICE AND AUTONOMOUS OPERATION

During maintenance periods of the main substation or loss of the main grid subsequent to a disturbance such as a permanent fault on the HV feeder, the power source in the distribution network of Fig. 1 is switched to the “temp-feeder”. The supply transfer is proven to cause voltage regulation and power-flow congestion problems due to the weak connection of the “temp-feeder”, [8]. The alternative approach is to form an island of part or of the entire backbone feeder when adequate local power generation is available. Islanding can improve reliability of the supply and voltage quality of the network. However, the slow response of the hydro-power generator and intermittent nature of the wind power generation sources can only support planned islanding of the network based on transition for a “close to zero power-flow” condition at the point of common coupling to the main grid. In addition, as discussed in [8], a 2-MVAr switched capacitor bank which is connected at the 25-kV side of the substation bus is anticipated to only partly compensate reactive power of the network during isolated operation. The above mentioned limitation of the available sources also affects load following capability of the network and limits the possibility of successful islanding and sustained autonomous operation to the time periods with high water levels for the run-of-river hydro-power generation, since it is the only controllable source.

### A. Annual energy balance

The RETScreen energy analysis model, [9], is used to determine annual energy production and consumption of the network. Table I shows the summary results for the energy balance of the network including energy production of the hydro power plant and the wind farm, and estimated energy consumption for residential and commercial loads. The hydro plant can operate at close to full generation capacity during the spring/summer irrigation period (May to October). Fig. 2 shows the water-flow duration curve and the maximum power

TABLE I

ANNUAL ENERGY BALANCE FOR THE UTILITY NETWORK OF FIG. 1

Power Generation			
Source	Rated Capacity (MW)	Annual Energy Production (MWh)	% of total Load
Hydro power	3	11,250.00	36.28%
Wind farm	3.78	9,064.00	29.23%
Utility grid	10	10,697.57	34.50%
Load Consumption			
Load	Rated Load (MW)	Annual Energy Consumption (MWh)	% of total Load
Residential	3.14	20,583.81	66.37%
Commercial	1.69	8,866.87	28.59%
System losses		1,560.89	5.03%

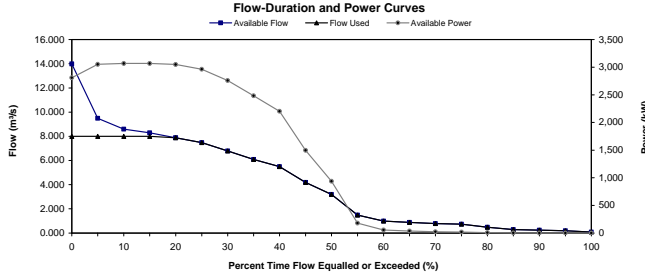


Fig. 2. Estimated annual flow and power generation curve for the hydro power generation

generation available for a typical year. A power generation of above 2500-kW can be expected 35% of the time on an annual basis, [9]. The average wind speed for the area of the wind farm installation is about  $5.4 \frac{m}{s}$  at 10-m height. For this wind speed, an annual energy production of 1800-MWh per 660-kW wind turbine is calculated. The utility grid supplies the balance of the energy (about 11-GWh/yr) mainly during the fall and winter periods when there is shortage of local generation.

### B. Planned islanding strategy

Monthly analyses of the power generation and consumption show that the daily power generation surpasses the load demand for several days in spring and summer when hydro-power plant has enough water resources to operate at full load. Under these conditions the power flow direction at the main substation is reversed to export the excess power to the utility grid. A pre-scheduled planned islanding operating scenario can be adopted during these periods by controlling the power generation of the hydro-power plant to reduce the real power-flow at the substation close to zero. The capacitor bank that is connected at the PCC is also controlled locally to compensate the reactive power of the network measured at the substation point. Prior to disconnection from the main grid, the control mode of the hydro power plan is also switched from a grid-following mode to a grid-forming mode that provides load-following capability and voltage regulation based on the governor and excitation system controls. Several cases of planned islanding operation are studied that show validity of the control strategy for an operating scenario with low penetration of wind power generation as reported in Section VI-A. However, under strong wind regimes and/or when the power flow at the PCC at

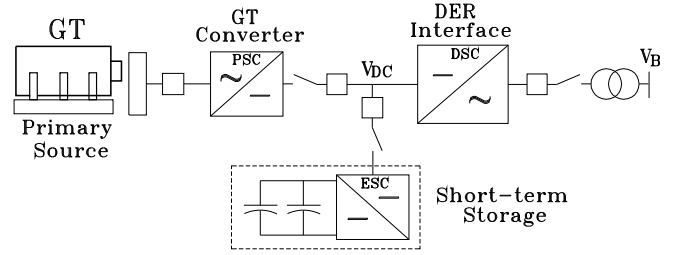


Fig. 3. Electronically-interfaced dispatchable DER (EID-DER)

the time of disconnection is greater than 5% of the generation capacity of the hydro-power source, the frequency and voltage excursions are beyond the acceptable ranges of  $\pm 1\%$  and  $\pm 3\%$ , respectively.

### C. Dispatchable DER

The implementation and interconnection of a fast-acting dispatchable source to the network is proposed as a solution for seamless islanding transition (planned and/or accidental islanding) and to manage power fluctuations of the intermittent sources during autonomous operation, [10]. The network can then be operated as a utility Microgrid.

Fig. 3 shows a block diagram representation of an electronically-interfaced dispatchable source (EID-DER) which is composed of the following: (i) a three-phase voltage source inverter equipped with real and reactive power controllers as the interface medium, (ii) an ultracapacitor energy storage module with a dc-to-dc converter for short-duration energy supply, (iii) a primary power generation source such as a gas turbine, (iv) a multifunctional control, monitoring, and communication system. The proposed EID-DER is connected to the backbone feeder at the main substation. A low-speed communication system is used to update the reference points for real/reactive power sharing and coordinate operation of EID-DER with the hydro-power generator. The major system quantities which are measured locally at the PCC and used as input parameters for the EID-DER controller are the power frequency and bus voltages.

## IV. DESIGN METHODOLOGY

The proposed design approach is based on the study of the dynamic performance of the system with available sources (wind and hydro) and investigation of the system stiffness. In this case, the hydro-power generator is the primary source of frequency and voltage control for the network. The transfer function model of the hydro power generator is developed for different frequency control strategies and is used to analyze frequency response characteristics. The transfer function model relates change in the frequency to real power mismatches in the network, which provides an analytical basis for the control system design of the EID-DER and sizing of the short-term energy storage. The analytical method to derive the system transfer function and design the EID-DER controls are briefly explained in the following subsections.

### A. Analytical model

The frequency control in a hydro-power generator is applied through a governor system. Two common frequency control methods are, [11]: (i) frequency-droop (speed-droop) method which adjusts the output power of the generator with an inverse function of the change in the power frequency, and (ii) frequency restoration method, also known as isochronous control, that attempts to restore the frequency to its reference point by varying the output power as a function of change in frequency. The frequency control methods are analytically represented by (1) and (2) which show the relationship between change in frequency and output power as follows:

1) Frequency droop method:

$$\omega_s = \omega_{ref} - D_r(P_m - P_{ref}), \quad (1)$$

2) Frequency restoration method:

$$\omega_s = \omega_{ref} - \frac{D_r s}{k_{r1}s + k_{r2}}(P_m - P_{ref}), \quad (2)$$

where  $D_r$  is the droop coefficient, and  $k_{r1}$  and  $k_{r2}$  are the frequency controller parameters. In (1) and (2),  $\omega_s$  and  $\omega_{ref}$  are the system frequency and the reference frequency, respectively; likewise  $P_m$  and  $P_{ref}$  are the actual and reference power values.

The swing equation describes electromechanical dynamics of a synchronous generator, its prime mover (here a hydro-turbine), and loads when either input power or electrical load is changed, [12]. Equation (3) provides a per-unit representation of the swing equation, as described in Appendix A, that relates variations in the input mechanical power and/or the output electrical power given by

$$2Hs\Delta\omega_s = \Delta P_m - \Delta P_e, \quad (3)$$

where  $H$  is the overall inertia constant of the turbine-generator set in seconds.  $\Delta P_m$  represents the change in mechanical power of the turbine-generator set which is controlled by the governor system. Assuming that the hydro-generator governor operates based on a frequency-droop method, a simplified turbine-governor transfer function that represents the relationship between the  $\Delta P_m$  and the frequency change is given by, [13],

$$\Delta P_m = -\frac{k_1}{s + k_2}\Delta\omega_s, \quad (4)$$

where  $k_1$  and  $k_2$  are constants related to the turbine time constant and the governor droop coefficient as follows:

$$k_1 = \frac{1}{\tau_g D_r} \text{ and } k_2 = \frac{1}{\tau_g}.$$

In (3),  $\Delta P_e$  is the variations in the electrical power of the system introduced by change in the load demand and/or the power mismatch due to sudden disconnection of a source. To obtain a closed-form representation for  $\Delta P_e$ , voltage and frequency dependency of the network components including loads and other sources needs to be considered. Hence, two cases are investigated: one with only the hydro generator connected to the network (without a dispatchable source), and the second case with EID-DER.

1) **Case I: Hydro generator without EID-DER:** The load-frequency dependency is represented by a damping factor  $D$  and the power mismatch is given by  $\Delta P_o$ . Substituting for  $\Delta P_m$  and  $\Delta P_e$  in the per-unit swing equation of (3) from turbine-transfer function of (4) and the load-frequency relationship, respectively; then re-arranging the equation yields

$$(2Hs + \frac{k_1}{s + k_2} + D)\Delta\omega_s = -\Delta P_o. \quad (5)$$

Hence, the transfer function model of the network is given by

$$\frac{\Delta\omega_s}{\Delta P_o} = \left(\frac{-1}{2Hs}\right) \frac{s + k_2}{s^2 + (k_2 + \frac{D}{2H})s + \frac{Dk_2 + k_1}{2H}}. \quad (6)$$

The closed-form transfer function of (6) is then used to characterize the rate and range of the frequency changes of the hydro-generator ( $\Delta\omega_s$ ) for a given value of real power mismatch ( $\Delta P_o$ ).

2) **Case II: Hydro generator with EID-DER:** In the per-unit swing equation of (13), Appendix A,  $p_e(t)$  represents the electrical load of the generator. For this case, the variations in  $p_e(t)$  is defined by three components:

$$\Delta P_e = \Delta P_L + \Delta P_{EDER} + \Delta P_o, \quad (7)$$

where  $\Delta P_L$  is the change in load,  $\Delta P_{EDER}$  represents the power supplied by the dispatchable source in response to frequency/voltage disturbances, and  $\Delta P_o$  is the power mismatch introduced by disconnection of a source or the utility grid, e.g. in the case of islanding. The closed-form representations of  $\Delta P_L$  and  $\Delta P_{EDER}$  are derived in Appendices B and C. Substituting for  $\Delta P_L$  and  $\Delta P_{EDER}$  from (18) and (19), respectively, in (7) yield

$$\Delta P_e = (K_L + \frac{k_{rp}s + k_{ri}}{s})\Delta\omega_s + \Delta P_o. \quad (8)$$

The transfer function model of the network for this case is formulated in the same manner as described for Case I by substituting  $\Delta P_m$  and  $\Delta P_e$ , given by (4) and (8), in the per-unit swing equation of (3). Hence,

$$\frac{\Delta\omega_s}{\Delta P_o} = \left(\frac{-1}{2Hs}\right) \frac{s(s + k_2)}{s^3 + (k_2 + \frac{K_L + k_{rp}}{2H})s^2 + \frac{k_1 + k_{ri}}{2H}s + \frac{(k_{ri} + K_L)k_2}{2H}} \quad (9)$$

where  $k_1$  and  $k_2$  are known values specified by the turbine-governor characteristic of the hydro-power generator and  $H$  is the inertia constant of the generator, while  $K_L$ ,  $k_{rp}$  and  $k_{ri}$  are the design parameters employed by the EID-DER controllers. The appropriate selection of these parameters determine the desired frequency response characteristic of the network for a given  $\Delta P_o$ . One approach to calculate the control parameters from (9) is to express the denominator of the transfer function in the following form

$$D(s) = (s + \alpha)(s^2 + 2\zeta\omega_n s + \omega_n^2) \quad (10)$$

where  $-\alpha$  is a desired pole for the closed-loop controller, and  $\zeta$  and  $\omega_n$  are the damping ratio and the natural frequency of a desired second-order characteristic function.

Once the EID-DER controllers are designed,  $\omega_s$  is determined for a presumed disturbance, for instance,  $\Delta P_o = 20\%$  using (9). Then, the power contribution of the energy storage

and an estimation of the total energy required to damp out power fluctuations are calculated as follows:

$$\Delta P_{ES} = \Delta P_{EDER} - \Delta P_{GT} \quad (11)$$

$$\Delta E_{ES} = \int_{\Delta T_s} \Delta P_{ES} dt, \quad (12)$$

where  $\Delta P_{ES}$  and  $\Delta P_{GT}$  are power contributions of the energy storage and the gas turbine during the disturbance, respectively.  $\Delta E_{ES}$  is the change in the internal energy of the ultracapacitor storage over a  $\Delta T_s$  period.  $\Delta T_s$  is defined by the response time of the gas turbine for a step-change in the real-power set point, which is normally in the range of 15 to 30 s. After estimating  $\Delta E_{ES}$ , the total capacitance of the energy storage and cells combinations can be determined based on a method described in [14] that uses the voltage discharge profile of the ultracapacitor storage to select the number of capacitor cells and the series/parallel configuration.

## V. CONTROL SYSTEM

The control system of EID-DER is designed based on the information extracted from the analysis of the dynamic behavior of the hydro-power generator, estimation of the frequency stabilization requirements and study of the gas-turbine power generation characteristic as the primary source. A schematic representation of the EID-DER configuration is shown in Fig. 4. The grid-interface converter of the dispatchable source (DSC) and the converter interface for the primary source (PSC) in Fig. 4 employ  $dq$ -control strategies for fast and decoupled control of real and reactive power, [15]. The full-bridge dc-to-dc converter of the energy storage (ESC) operates in a current-controlled mode to supply instantaneous current needed to regulate the  $dc$  link voltage, while maintaining a minimum capacitor voltage. The gas turbine is equipped with governor and excitation controls to adjust the real power output and terminal voltage, respectively. A power dispatch controller for the local distribution network specifies the base power of the gas-turbine ( $P_{GT}^o$ ) according to load variations, the average wind power generation, and the reserve capacity of the hydro generator. The control strategies for the DSC and PSC controllers are described in the following subsections.

### A. DSC Control

Fig. 5 shows the block diagram for real and reactive power control of the dispatchable source converter (DSC). The real power control circuitry responds to variations in system frequency. The input to the block is the local frequency ( $\omega_s$ ), estimated by a conventional PLL using bus voltages, Fig. 5(a). The output of the block is the reference current for the  $d$ -axis inner current controller of the unit,  $i_d(DS)$ , corresponding to the real power reference of the unit ( $P_{ref}$ ). The real power reference for DSC is composed of three terms: (i) a term corresponding to the variations in the power frequency determined by the frequency restoration block, (ii) the second term that is proportional to changes in the bus voltage for damping, Appendix B, and (iii) the third term corresponding to the power dispatch value assigned to the gas turbine unit ( $P_{GT}^o$ ), Fig. 5(a).

Voltage regulation during islanding operation is performed by the hydro-power generator since it operates based on a grid-forming strategy. Therefore, a reactive power compensation strategy is adopted for the DSC control. Fig. 5(b) shows a reactive power control strategy based on voltage-droop characteristic including a pre-set V-Q characteristic to determine reactive power reference  $Q_{ref}$  of the unit, and a  $PI$  controller to assign the  $q$ -axis current  $i_q(DS)$ . The input to the block is the rms value of the voltage at the point of connection of the EID-DER (PCC). The  $PI$  controller specifies the corresponding  $q$ -axis current set-point to adjust the reactive power generation of the unit,  $Q_{DS}$ , based on the difference between the reference value determined from the Q-V curve and the reactive power injection of the switched-capacitor banks, represented by  $Q_{ext}$ , Fig. 5(b). Thus, reactive power of the EID-DER varies based on deviations in the bus voltage. The step-changes for reactive power compensation are applied through the capacitor banks, while the fine-tuning is provided by the DSC reactive power control.

### B. PSC Control

The  $d$  and  $q$  components of the primary source converter (PSC) are controlled to regulate the  $dc$ -link voltage and maintain the reactive power exchange with the gas-turbine generator, respectively. Fig. 6 shows the block diagram for  $dc$ -link voltage regulator and the reactive power control. Dynamic behavior of the  $dc$ -link voltage based on the power balance principle among a primary source, energy storage components of the  $dc$  and  $ac$  links, and the load is explained in [16]. A similar approach is adopted in the design of the  $dc$ -link controller of the EID-DER as shown in Fig. 6(a). The  $dc$ -link voltage regulator uses a  $PI$  controller to determine the reference value for the  $d$ -axis component of the PSC current,  $i_d(PS)$ , based on the variations in  $V_{DC}$ . Two feedforward components are added to the controller output to enhance steady-state and transient response of the controller. The feedforward current terms correspond to: (i) the real-power dispatch of the gas-turbine ( $P_{GT}^o$ ) to represent real power exchange between the primary source and the network through the voltage regulation of the  $dc$  link, and (ii) the instantaneous power of the energy storage ( $\Delta P_{ES}$ ) that compensates for slow response of the primary source during sudden changes. Fig. 7 shows the block diagram of the controller and ultracapacitor model for calculation of  $\Delta P_{ES}$ .

The reactive power controller for the PSC is shown in Fig. 6(b) that operates based on a reactive power compensation mode to determine the reference value for the  $q$ -axis component of the PSC current,  $i_q(PS)$ . The input to the controller is the reference reactive power,  $Q_{GT}$ , equivalent to reactive power exchange with the gas-turbine generator. This value is set to zero if operation at the unity power factor is required.

## VI. STUDY CASES

Several case studies are performed to investigate the dynamic responses and transients of the study distribution system subsequent to a planned islanding and/or an accidental islanding. Two case studies are reported in the following subsections

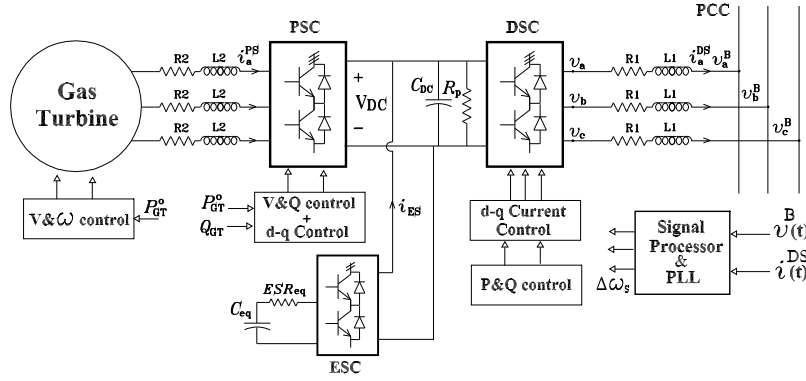


Fig. 4. A schematic representation of the EID-DER configuration

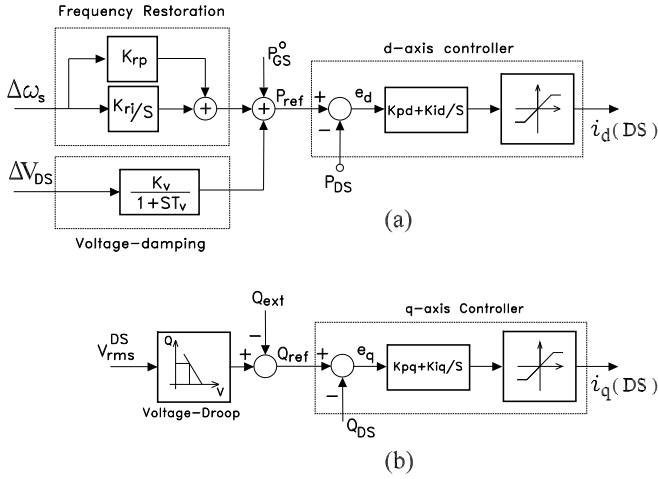


Fig. 5. Real and reactive power controllers for the grid-interface converter of the dispatchable source: a) Real power control, b) Reactive power control

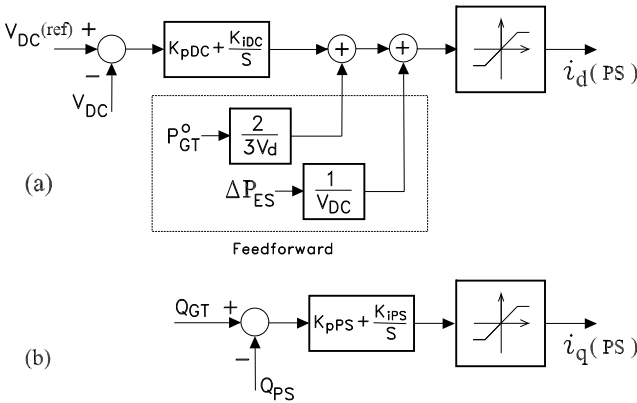


Fig. 6. dq-controls for the primary source converter interface: a) dc-link voltage regulator, b) Reactive power control

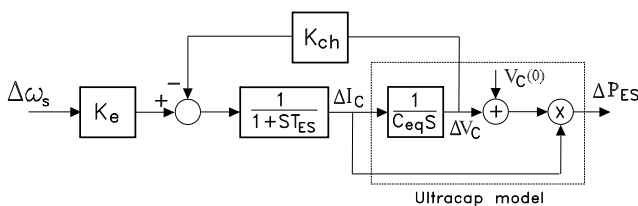


Fig. 7. Control block of the ultracapacitor energy storage

TABLE II

CONTROL PARAMETERS FOR THE EID-DER AND THE HYDRO GENERATOR

Hydro Gen.		DSC Control			
Dr	0.04	Krp	0.2	Kpd	0.012
Tg	1.1 s	Kri	83.3	Kid	1818.18
H	1.5 s	Kv	0.1	Kpq	0.012
ESC		Tv	0.026 s	Kiq	1818.18
Ke	1.67	ζ	0.7	ωn	9.5 rad/s
TES	0.082 s	PSC Control			
Kch	0.731	KpDC	1	KpPS	1.3
Ceq	38 F	KiDC	2.5	KiPS	50

Note: Time constants are in second, and gains are in per-unit of a 3.5-MVA, 25-kV base

that examined the islanding and autonomous operation without the EID-DER and in presence of the EID-DER. The studies are performed employing a digital computer simulation approach using the PSCAD/EMTDC software package.

#### A. Case-I: Planned islanding without EID-DER

Fig. 8 illustrates the response of the system of Fig. 1 to a planned islanding scenario as described in Section III-B. The hydro-power generator is the primary source of real and reactive power supply during islanding operation whose control mode is changed to the grid-forming strategy to regulate system voltage and provide load following capability. A low wind power generation condition based on an average wind speed of about  $5.5 \frac{m}{s}$  is assumed. However, a wind regime typical to the local area composed of several terms including wind turbulence, wind gust and randomly-generated noise components is used to simulate wind power fluctuations similar to the real system operation. Initially, the hydro-power generator supplies about 1.4-MW/0.6-MVar; the wind farm generates an average real power of about 0.5-MW and absorbs 0.27-MVar of reactive power. The utility grid, through the “main substation” delivers the balance of the power (about 0.4-MW/0.75-MVar). The grid also compensates for power fluctuations of the wind farm; therefore, the hydro-power generator operates at constant power, Figs. 8(c) and (d). The capacitor bank connected at the PCC is not in operation.

At  $t=20$  s, the planned islanding strategy of the system is activated by which the real power of the hydro-power generator is controlled to reduce the real-power import from

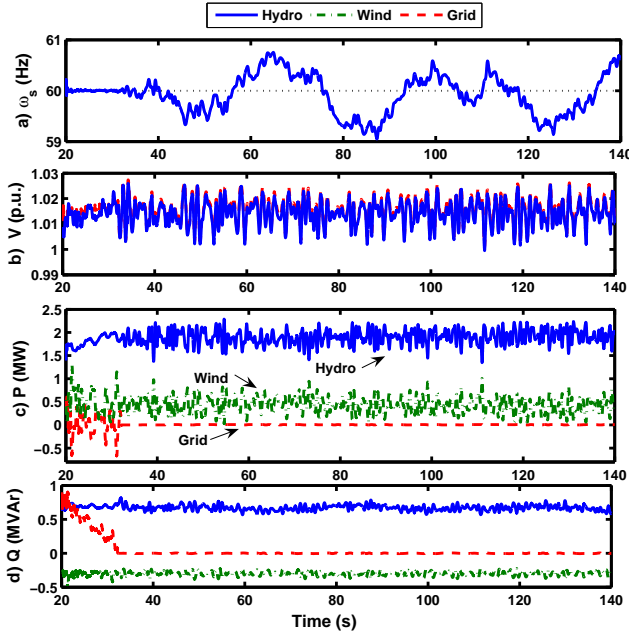


Fig. 8. Planned islanding of the study distribution system for Case-I without EID-DER: a) system frequency, b) rms voltage at PCC and Hydro-power generator terminal, c) real power of the local sources and the grid, d) reactive power of the sources and the grid

the grid to close to zero, Fig. 8(c). The capacitor bank, which is connected at the PCC, is also switched in and adjusted to gradually reduce the reactive power required from the grid as shown in Fig. 8(d). It should be noted that the capacitor switching time is shortened for the simulation purpose, for which the reactive power compensation process occurs in 12 seconds in comparison to a more realistic duration of several minutes. The main circuit breaker (CB1), Fig. 1, is disconnected when both real and reactive power flows from the grid are below 5% of the hydro-generator capacity, i.e. 150-kVA. Fig. 8(a) shows that after disconnection from the grid, at about  $t=32$  s, the power frequency represented by the rotational speed of the hydro-power generator undergoes large fluctuations with a maximum variation in the range of  $\pm 1.0$  Hz. However, the hydro-power generator can properly respond to power variations introduced by sudden changes in the wind speed, Figs. 8(c) and (d). The system voltage is maintained within a  $\pm 3\%$  of the rated voltage, although larger variations are observed compared to the grid-connected operation, Fig. 8(b). As shown in Fig. 8, planned islanding and autonomous operation without any energy storage or fast-acting dispatchable source is only feasible for low- and/or no-wind power contribution, where the hydro-power generator can maintain the voltage and frequency stability of the autonomous grid. The range of the frequency and voltage deviations may not be tolerable when there is significant amount of wind power fluctuations.

### B. Case-II: Islanding with EID-DER

This case examines the islanding transitions and autonomous operation of the distribution system in Fig. 1 for the similar loading and wind speed conditions as those of

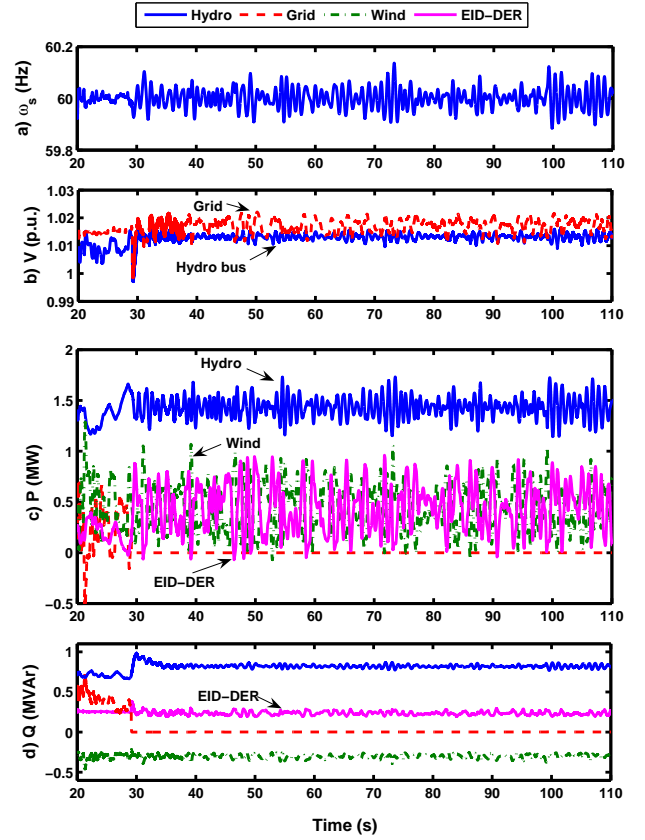


Fig. 9. Islanding transition and autonomous operation for Case-II with an EID-DER: a) system frequency, b) rms voltage at PCC and Hydro-power generator terminal, c) real power of the local sources and the grid, d) reactive power of the sources and the grid

Case-I. However, an EID-DER unit rated at 1-MVA is connected at the PCC. The EID-DER is composed of a 800-kW, 660-V gas-turbine generator and a 250-kW, 20-second (5-MJ) ultracapacitor energy storage as the primary and the secondary sources, respectively. The energy storage size and the control parameters are determined based on the approach in Section IV. The EID-DER specifications and the controllers' parameters are given in Table II.

Fig. 9 shows the system response for an islanding scenario and the subsequent autonomous operation supported by the fast acting EID-DER. In this case, after activation of the islanding control strategy, the real/reactive power flow at the PCC is monitored and adjusted to below 20% of the hydro-power generator capacity. Figs. 9(a) and (b) show that, after disconnection, despite power fluctuations of the wind turbines, the power frequency is maintained within  $\pm 0.2$ -Hz and the voltage variations are kept within an acceptable range of  $\pm 3\%$ . As shown in Figs. 9(c) and (d), the sudden changes in the real and reactive power of the wind farm are mainly compensated by the variations in the EID-DER power outputs; therefore, less fluctuations are observed by the hydro-power generator. Hence, the system voltage and frequency is controlled in the desired ranges even for an islanding transition with high power mismatch compared to Case-I ( $\Delta P_o = 20\%$ ).



## VII. CONCLUSIONS

The paper examined planned islanding and autonomous operation of part of a medium voltage distribution network. The islanded portion of the network was supplied by a hydro-power generator in the presence of a wind farm with low power penetration. A planned islanding strategy based on zero-power flow control at the PCC was discussed and investigated that showed the hydro-power generator's capability in sustaining the autonomous operation despite power fluctuations of the wind farm. However, it was shown that a fast-acting dispatchable DER is needed to sustain the island when there is a significant power mismatch at the time of disconnection and/or large power fluctuations caused by the wind farm. A design methodology based on frequency characterization of the system was introduced and used to determine the control parameters and the short-term energy storage size for an electronically-interfaced dispatchable DER. The simulation results from two case studies for the islanding operation with and without the dispatchable DER were presented that illustrate performance enhancement when using the dispatchable source.

## APPENDIX A

The per-unit swing equation that determines electromechanical dynamics of a turbine-generator motion is determined by:

$$\frac{2H}{\omega_{base}} \omega_{sp.u.}(t) \frac{d\omega_s(t)}{dt} = p_{mp.u.}(t) - p_{ep.u.}(t) \quad (13)$$

where  $\omega_{base} = 2\pi 60 \frac{rad}{s}$  is the base frequency and  $\omega_s(t)$  is the rotational speed of the generator shaft also in  $\frac{rad}{s}$ . Equation (13) is nonlinear because of the term with  $\omega_{sp.u.}(t)$  on the left side of the equation. Hence, the small-signal representation of (13) is obtained as follow. Applying small variations in  $\omega_s$ ,  $p_m$ , and  $p_e$  yields

$$2H(\omega_s(0) \frac{d\Delta\omega_s(t)}{dt} + \Delta\omega_s(t) \frac{d\omega_s(0)}{dt}) = \Delta p_m(t) - \Delta p_e(t) \quad (14)$$

where all quantities are in p.u. except H. Substituting the steady state values for  $\omega_s(0) = 1$  and  $\frac{d\omega_s(0)}{dt} = 0$  in (14) leads to:

$$2H \frac{d\Delta\omega_s(t)}{dt} = \Delta p_m(t) - \Delta p_e(t) \quad (15)$$

## APPENDIX B

The real power variations of the load is a function of voltage and frequency changes given by:

$$\Delta P_L = \frac{\partial P_L}{\partial V_m} \Delta V_m + \frac{\partial P_L}{\partial \omega_s} \Delta \omega_s \quad (16)$$

where  $\frac{\partial P_L}{\partial V_m} = D_v$  and  $\frac{\partial P_L}{\partial \omega_s} = D_\omega$  are defined as load-voltage and load-frequency sensitivity (damping) factors, respectively [13]. The damping factors are either constant values or in turn functions of the voltage and power frequency, depending on the load type. To derive the closed-form frequency transfer function for the case of the hydro-generator with EID-DER, it is assumed that changes in load voltage ( $\Delta V_m$ ) is incorporated in the real-power controller of the dispatchable source and controlled as a linear function of  $\Delta \omega_s$ . That is:

$$\Delta V_m = K_v \Delta \omega_s \quad (17)$$

Substituting for  $\Delta V_m$  from (17) in (16) and re-arranging this equation yields

$$\Delta P_L = K_L \Delta \omega_s \quad (18)$$

where  $K_L = (D_L K_v + D_\omega)$ .

## APPENDIX C

A fast frequency restoration strategy is adapted to an electronically-interfaced dispatchable source that operates in a similar manner as an isochronous governor control method for a conventional rotating generator. The frequency restoration method is described by (2). The real power variation of the EID-DER is then given by

$$\Delta P_{EDER} = \left( \frac{k_{rp}s + k_{ri}}{s} \right) \Delta \omega_s, \quad (19)$$

where  $k_{rp}$  and  $k_{ri}$  are the proportional and integral gains of the frequency controller.

## ACKNOWLEDGEMENT

The authors would like to thank Mr. Richard Bahry (Fortis Alberta) for providing benchmark data and his constructive comments.

## REFERENCES

- [1] H. You *et al.*, "Self-healing in power systems: an approach using islanding and rate of frequency decline-based load shedding," *IEEE Trans. Power Syst.*, vol. 18, no. 1, pp. 174–181, Feb. 2002.
- [2] R. Fulton and C. Abbey, "Planned islanding of 8.6 MVA IPP for BC Hydro system reliability," in *First International Conference on the integration of RE and DER*, Dec. 2004, pp. 1–9.
- [3] S. Ahmed *et al.*, "A scheme for controlled islanding to prevent subsequent blackout," *IEEE Trans. Power Syst.*, vol. 18, no. 1, pp. 136–143, Feb. 2002.
- [4] M. A. Schwake and B. Staib, "Recent progress in ultracaps for automotive applications," in *Proc. the 2nd AABC Conference*, Las Vegas, USA, 2002.
- [5] A. Rufer, D. Hotellier, and P. Barrade, "A supercapacitor-based energy storage substation for voltage compensation in weak transportation networks," *IEEE Trans. Power Delivery*, vol. 19, no. 2, pp. 629–636, Apr. 2004.
- [6] R. Jain, K. K. Ramakrishnan, and D. M. Chiu, "Capacitor-stabilized soft-transfer interface system for distributed resources," Electric Power Research Institute (EPRI), Palo Alto, CA, Tech. Rep. report # 1003970, Feb. 2002.
- [7] C. McKay, "Ultracapacitor EnergyBridge<sup>TM</sup> UPS for Palmdale water district," in *Proc. the second EESAT conference*, California, USA, 2005.
- [8] F. Katiraei, C. Abbey, and R. Bahry, "Analysis of voltage regulation problem for a 25-kV distribution network including distributed generation," in *Proc. IEEE PES General Meeting 2006*, Montreal, Canada, June 2006.
- [9] (2006) Wind and small-hydro energy project models. [Online]. Available: <http://www.retscreen.net/ang>
- [10] F. Katiraei, M. R. Iravani, and P. W. Lehn, "Micro-grid autonomous operation during and subsequent to islanding process," *IEEE Trans. Power Delivery*, vol. 20, no. 1, pp. 248–257, Jan. 2005.
- [11] R. M. Wright, "Understanding modern generator control," *IEEE Trans. Energy Conversion*, vol. 4, no. 3, pp. 453–458, Sept. 1989.
- [12] P. C. Krause, *Analysis of Electric Machinery and Drive Systems*. IEEE Press, 2002.
- [13] P. Kundur, *Power System Stability and Control*. New York: McGraw-Hill, 1994.
- [14] H. Douglas and P. Pillay, "Sizing ultracapacitor for hybrid electric vehicles," in *Proc. Industrial Electronics Conference IECON 2005*, vol. 2005, 2005, paper 1569143, pp. 1599–1604.
- [15] C. Schauder and H. Mehta, "Vector analysis and control of the advanced static VAR compensators," in *IEEE Proc. Generation, Transmission and Distribution*, vol. 140, no. 4, July 1993, pp. 299–306.
- [16] A. Yazdani and R. Iravani, "Control of high-performance switched-mode rectifier system," *the IEE Proceeding of Electric, Power Applications*, vol. 152, no. 6, pp. 1451–1458, Nov. 2005.